iScience, Volume *23*

Supplemental Information

Hyperexcitable Parvalbumin Interneurons Render Hippocampal Circuitry Vulnerable to Amyloid Beta

Sara Hijazi, Tim S. Heistek, Rolinka van der Loo, Huibert D. Mansvelder, August B. Smit, and Ronald E. van Kesteren

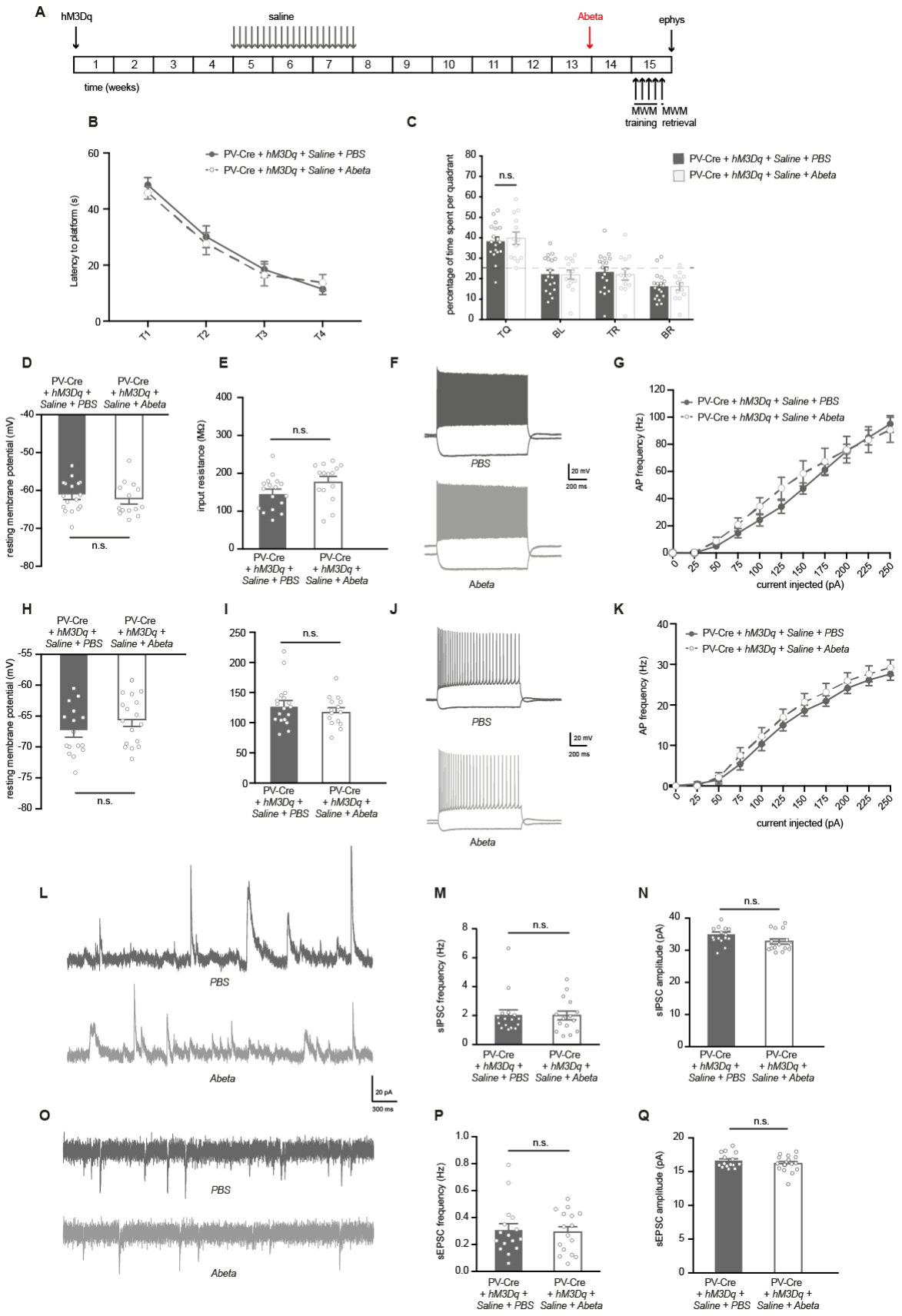

Figure S1, related to Figure 4. A single low dose of amyloid beta has no effect on spatial memory, neuronal properties or synaptic transmission in saline-treated control mice. (**A**) PV-Cre mice were injected with hM3Dq virus at 8-10 weeks of age. After 4 weeks, saline was i.p. injected daily for a period

of 3 weeks. Bilateral infusion of 0.15 fmole of Ab oligomers or PBS control in the CA1 region of the hippocampus of PV-Cre mice was done 6.5 weeks after discontinuation of saline injections. A MWM test was performed 1.5 week after Ab infusions. Electrophysiological recordings were performed following the MWM test. (**B**) Spatial learning was assessed measuring the latency to find the hidden platform on 4 consecutive training days (T1-4). Both Ab-infused and PBS-infused PV-Cre mice showed significant learning during training (*training* two-way repeated measures ANOVA: n = 18/13 per group, $F_{3,72}$ = 47.65, $p < 0.001$). (**C**) During the one-minute probe trial, both groups spent significantly more time in the target quadrant (TQ), which was higher than chance level (dashed line) and there was no difference detected between groups (two-way ANOVA: n=18/13 mice per group, $F_{3, 87}$ = 0.09, p = 0.960). (**D**) PV interneuron resting membrane potential was unaltered between groups (Student's t test: n = 17/15 cells from 4 mice per group, p = 0.502). (**E**) There was no difference in PV interneuron input resistance between Ab-infused and PBS-infused PV-Cre mice (Student's t test: n = 17/15 cells from 4 mice per group, p = 0.069). (**F**) Voltage responses to 1 s hyperpolarizing or depolarizing current steps from a PV interneuron in PBS-infused (grey) and Ab-infused (light grey) PV-Cre mice. (**G**) Average action potential (AP) frequency in response to 0-250 pA depolarizing current steps illustrating no change in PV interneuron firing frequency in Ab-infused compared to PBS-infused PV-Cre mice (*group x current* two-way repeated measures ANOVA: n = 17/15 cells from 4 mice per group, $F_{10,300}$ = 1.29, p = 0.238). (**H**) Pyramidal neuron resting membrane potential was also unaltered in Ab-infused compared to PBS-infused PV-Cre mice (Student's t test: n = 17/16 cells from 4 mice per group, p = 0.222). (**I**) Pyramidal neuron input resistance was not changed between groups (Student's t test: n = 17/16 cells from 4 mice per group, p = 0.366). (**J**) Voltage responses to 1 s hyperpolarizing or depolarizing current steps from a pyramidal neuron in PBS-infused (grey) and Ab-infused (light grey) PV-Cre mice. (**K**) AP frequency in response to 0-250 pA depolarizing current steps showing no difference in pyramidal neuron excitability in Ab-infused compared to PBS-infused PV-Cre mice (*group x current* two-way repeated measures ANOVA: n = 17/16 cells from 4 mice per group, $F_{10,280}$ = 0.819, p = 0.611). (**L**) Example traces of spontaneous inhibitory postsynaptic currents (sIPSC) recorded from hippocampal pyramidal neurons in PBS-infused (grey) or Ab-infused (light grey) PV-Cre mice. (**M-N**) No significant alterations were observed in the frequency (**M**) or in the amplitude (**N**) of sIPSCs in Ab-infused compared to PBS-infused PV-Cre mice (Mann-Whitney test: n = 16/15 cells from 4 mice per group, p = 0.985 and p = 0.060). (**O**) Example traces of spontaneous excitatory postsynaptic currents (sEPSC) recorded from hippocampal pyramidal neurons in PBS-infused (grey) or Ab-infused (light grey) PV-Cre mice. (**P-Q**) No significant alterations were observed in the frequency (**P**) or in the amplitude (**Q**) of sEPSCs in Ab-infused compared to PBS-infused PV-Cre mice (Mann-Whitney test: n = 16 cells from 4 mice per group, p = 0.955 and p = 0.654).

Table S1, related to Figure 2. Passive and active membrane properties of hippocampal PV interneurons and pyramidal neurons in saline and CNO-injected hM3Dq-expressing WT-PV-Cre mice (Early time-point).

	PV interneurons					Pyramidal neurons				
	Saline		CNO		*p-value*	Saline		CNO		*p-value*
Properties	(mean	± SEM)	(mean	± SEM)	(Student's *t*-test)	(mean	± SEM)	(mean	± SEM)	(Student's *t*-test)
Passive properties										
Vm (mV)	-63.2	0,89	-62,3	0,92	0,514	-64,1	0,76	-64,9	0,76	0,437
sagV (mV)	-1,6	0,38	-1,4	0,29	0,759	-1,9	0,16	-2,3	0,28	0,162
taufit (ms)	17,6	1,84	22,1	2,45	0,177	11,7	0,64	11,6	0,90	0,997
Rinput (Mohm)	138,8	10,01	187,6	15,39	0,018	100,9	5,37	96,4	4,42	0,534
Active properties										
AP frequency at 250 pA (Hz)	83,0	8,61	98,9	3,66	0,036	23,8	1,82	24,0	1,40	0,927
AP threshold (mV)	-48,7	1,42	-48,1	0,77	0,701	-48,2	0,56	-47,8	1,10	0,738
AP amplitude (mV)	77,1	2,00	72,8	2,02	0,151	102,3	1,55	97,8	2,61	0,140
AP half-width (msec)	0,41	0,02	0,48	0,02	0,013	1,4	0,04	1,5	0,07	0,067
AHP (mV)	17,9	1,19	19,7	0,74	0,227	8,3	0,75	6,7	0,89	0,175
adaptation	0,91	0,13	0,76	0,09	0,344	0,93	0,05	0,93	0,05	0,978
Rheobase	70,6	11,79	47,9	4,23	0,048	123,9	7,07	126,3	6,66	0,808

Table S2, related to Figure 3. Passive and active membrane properties of hippocampal PV interneurons and pyramidal neurons in saline and CNO-injected hM3Dq-expressing WT-PV-Cre mice (Late time-point).

	PV interneurons					Pyramidal neurons				
	Saline		CNO		*p-value*	Saline		CNO		*p-value*
Properties	(mean	± SEM)	(mean	± SEM)		(mean	± SEM)	(mean	± SEM)	
Passive properties										
Vm (mV)	-66,3	0,52	-66,5	0,46	0,778	-66,8	0,49	-68,3	0,81	0,122
sagV (mV)	-1,8	0,47	-3,7	0,73	0,042	-3,0	0,29	-4,0	0,39	0,043
taufit (ms)	17,8	1,30	28,5	2,66	0,002	18,6	1,36	23,6	1,91	0,040
Rinput (Mohm)	125,2	8,58	192,4	12,22	0,000	118,8	8,54	142,8	6,48	0,031
Active properties										
AP frequency at 250 pA (Hz)	57,0	4,99	72,9	4,16	0,020	15,9	1,03	18,7	0,90	0,025
AP threshold (mV)	-50,1	1,87	-48,7	1,07	0,496	-46,6	0,94	-47,1	1,60	0,774
AP amplitude (mV)	78,5	2,95	84,3	2,98	0,189	108,9	1,18	101,0	1,99	0,001
AP half-width (msec)	0,74	0,04	0,67	0,03	0,179	2,29	0,04	2,22	0,07	0,440
AHP (mV)	15,1	1,43	18,3	0,78	0,042	6,3	0,40	7,5	0,93	0,245
adaptation	0,69	0,12	1,29	0,39	0,211	0,82	0,08	0,66	0,10	0,191
Rheobase	91,7	5,62	70,0	6,44	0,006	93,5	8,20	70,7	6,41	0,025

Table S3, related to Figure S1. Passive and active membrane properties of hippocampal PV interneurons and pyramidal neurons in saline -injected hM3Dq-expressing WT-PV-Cre mice after Abeta infusions.

	PV interneurons					Pyramidal neurons				
	Control		Abeta		*p-value*	Control		Abeta		*p-value*
Properties	(mean	± SEM)	(mean	± SEM)	(Student's *t*-test)	(mean	± SEM)	(mean	± SEM)	(Student's *t*-test)
Passive properties										
Vm (mV)	-61,3	1,01	-62,3	1,18	0,502	-67,5	0,99	-65,7	0,95	0,222
sagV (mV)	-2,2	0,34	-1,4	0,24	0,062	-2,3	0,26	-2,9	0,39	0,211
taufit (ms)	17,4	1,85	19,2	1,89	0,511	14,8	1,02	12,6	0,66	0,100
Rinput (Mohm)	147,9	10,74	179,1	12,71	0,069	128,5	8,30	118,6	6,42	0,366
Active properties										
AP frequency at 250 pA (Hz)	95,0	6,21	90,7	9,25	0,697	27,7	1,59	29,2	1,94	0,545
AP threshold (mV)	-43,1	1,79	-44,3	1,91	0,650	-51,4	0,98	-52,0	1,05	0,672
AP amplitude (mV)	56,7	1,77	59,0	2,97	0,507	96,3	1,43	97,1	2,33	0,759
AP half-width (msec)	0,45	0,02	0,47	0,02	0.539	1,31	0,03	1,28	0,05	0,606
AHP (mV)	17,1	1,42	17,6	1,28	0.787	7,8	0,54	8,2	0,65	0,627
adaptation	0,94	0,09	1,29	0,26	0,207	0,94	0,03	0,89	0,05	0,427
Rheobase	80,9	8,98	83,3	12,83	0,874	81,9	6,94	83,3	9,34	0,904

Table S4, related to Figure 4. Passive and active membrane properties of hippocampal PV interneurons and pyramidal neurons in CNO -injected hM3Dq-expressing WT-PV-Cre mice after Abeta infusions.

	PV interneurons					Pyramidal neurons				
	Control		Abeta		*p-value*	Control		Abeta		*p-value*
Properties	(mean	± SEM)	(mean	± SEM)	(Student's *t*-test)	(mean	± SEM)	(mean	± SEM)	(Student's *t*-test)
Passive properties										
Vm (mV)	-62,0	1,21	-57,4	0,90	0,005	-65,0	1,04	-63,7	0,82	0,300
sagV (mV)	-2,8	0,55	-2,9	0,80	0,920	-2,5	0,25	-2,0	0,19	0,185
taufit (ms)	16,8	1,41	14,2	1,42	0,209	12,4	0,89	10,7	0,64	0,130
Rinput (Mohm)	142,9	8,85	136,0	17,44	0,740	101,6	5,93	85,8	5,95	0,070
Active properties										
AP frequency at 250 pA (Hz)	100,0	7,77	74,1	11,01	0,003	22,9	1,12	30,2	1,81	0,000
AP threshold (mV)	-44,7	0,84	-46,0	1,24	0,405	-49,3	1,10	-50,6	0,35	0,287
AP amplitude (mV)	66,4	1,63	73,1	4,20	0,172	103,4	2,15	105,5	1,93	0,492
AP half-width (msec)	0,43	0,02	0,52	0,06	0,177	1,41	0,06	1,01	0,02	0,000
AHP (mV)	16,6	0,92	14,2	1,26	0,136	5,6	0,42	7,0	0,51	0,040
adaptation	0,92	0,04	0,97	0,06	0,517	0,89	0,05	0,88	0,06	0,910
Rheobase	88,8	10,49	97,1	15,59	0,653	123,5	8,95	107,4	9,29	0,219

Transparent Methods

Animals

The PV-Cre mouse strain used was originally purchased from the Jackson Laboratory (# B6.129P2-Pvalbtm1(cre)Arbr/J; stock number 017320) and expresses Cre recombinase under the parvalbumin (Pvalb) promoter, inducing Cre expression specifically in parvalbumin expressing cells as reported in (Hippenmeyer et al., 2005). All experiments were performed with single-housed male mice and approved by the Central Committee for Animal Experiments (CCD) and the Animal Welfare Body (IVD) of the VU University Amsterdam.

Virus

Floxed mCherry (hSyn-DIO-mCherry) and floxed hM3Dq-mCherry (hSyn-DIO-hM3Dq-mCherry) AAVs (1012 vc/ml) were packaged as serotype 5 virus.

Stereotaxic surgeries

All surgeries were done as described previously in (Hijazi et al., 2019). The CA1 region was targeted bilaterally using the following coordinates: AP: -1.7 mm, DV: -1.7 mm, ML: ± 1.1 mm. A volume of 0.5 µL for AAV and 0.3 µL for Ab oligomers was infused using a thin glass needle and a 10 µL Hamilton needle syringe at a rate of 0.1 µL/min. Mice were single-housed and experiments were conducted 4 weeks post-surgery.

Chemogenetic manipulation of PV interneurons

Mice were injected intraperitoneally with either 0.9% saline or with clozapine-N-oxide (CNO) dissolved in 0.9% saline. For Figure 1J-L, mice received CNO (2 mg/kg) 30 min prior to each training session in the Morris water maze. For the rest of the CNO injections, mice received daily CNO (1 mg/kg) for 3 weeks. Behavioral or electrophysiological testing were conducted 48 hours or 8-10 weeks after the last CNO injection.

Slice preparation and electrophysiology

All electrophysiological experiments were done as described in (Hijazi et al., 2019). Briefly, brains were rapidly removed and hippocampal coronal slices of 300µm thickness were prepared in ice-cold partial sucrose solution containing (in mM): sucrose 70, NaCl 70, $NaHCO_3$ 25, KCl 2.5, NaH_2PO_4 1.25, $CaCl_2$ 1, $MgSO_4$ 5, sodium ascorbate 1, sodium pyruvate 3 and D(+)-glucose 25 (carboxygenated with 5% CO_2 / 95% O_2). The slices were left to recover for 30 min in 34 °C holding aCSF containing (in mM): NaCl 125, $NaHCO_3$ 25, KCl 3, NaH_2PO_4 1.2, $CaCl_2$ 1.3, $MgSO_4$ 1, $MgCl_2$ 1, sodium pyruvate 3, sodium ascorbate 1 and D(+)-glucose 25 (carboxygenated with 5% CO_2 / 95% O_2). Following recovery, slices were left for at least 1 hour in holding ACSF at room temperature. PV cells were recognized by mCherry fluorescence. Slices were then moved to the recording chamber and continuously perfused with standard ACSF at 34^{o}C containing (in mM): NaCl 125, $NaHCO_3$ 25, KCl 3, NaH_2PO_4 1.2, $CaCl_2$ 1.3, $MgSO_4$ 1and D(+)-glucose 25 (carboxygenated with 5% CO_2 / 95% O_2).

All neurons were recorded in whole-cell mode using a Multiclamp 700B amplifier (Molecular Devices, Sunnyvale, CA). Borosilicate glass electrodes (Harvard Apparatus, Holliston, MA) with tip resistances of 2–5 MOhm. For spontaneous events, the intracellular solution was composed of (in mM): Cs-gluconate 125, CsCl 5, HEPES 10, K-phosphocreatine 10, ATP-Mg 2, and GTP 0.3 EGTA 0.2 QX314 1 (pH adjusted to 7.2 with CsOH) and for all recordings in current-clamp: K-gluconate 135, HEPES 10, K2-phosphocreatine 10, ATP-Mg 2, NaCl 4, EGTA 0.2 and GTP 0.3 (pH adjusted to 7.2 with KOH). Resting membrane potential was measured directly after obtaining whole-cell configuration. Intrinsic properties were obtained in current-clamp mode by injecting 1-ms of increasing current stimuli. Cells were clamped at -65 mV and at -70 mV for PV neurons and pyramidal neurons respectively. Access resistance was monitored throughout the recordings. Neurons with access resistance that was above 25 MOhm or neurons that displayed unstable resting membrane potential or aberrant spiking pattern were excluded from the analysis. Data analysis was performed using a custom-designed script in Igor Pro-7.0 (Wavemetrics). IPSCs were recorded at 0 mV holding potential. EPSCs were recorded at -70 mV holding potential. Synaptic events were detected using Mini Analysis Program (Synaptosoft, Decatur, GA).

Tissue preparation and immunohistochemistry
Staining was performed on free-floating brain sections as previously described (Vegh et al., 2014). The blocking solution was composed of 0.2% (v/v) Triton X-100 and 5% (v/v) fetal bovine serum in PBS. The slices were incubated overnight with mouse anti-PV (Millipore, Billerica, MA, MAB 1572; 1:1000) for PV staining or rabbit anti-cFos (Synaptic Systems; 1:1000) for cFos staining. PV and cFos staining were visualized using anti-mouse Alex568 and anti-rabbit Alexa488-labeled secondary antibodies (Invitrogen, Carlsbad, CA; 1:400), incubated for 2 hours at RT. Slices were coverslipped in Vectashield with DAPI as a nuclear dye (Vector Laboratories, Burlingame, CA). All images were acquired on a Nikon confocal microscope, using the same objective, exposure time, gain settings and camera settings for all images from the same experiment. PV and cFos-positive cells were quantified using ImageJ v1.48.

Preparation of Aβ oligomers
HFIP-treated $A\beta_{1-40}$, $A\beta_{1-42}$ peptides were obtained from Bachem and prepared as described previously (Stine et al., 2011). Shortly, the peptides were dissolved in DMSO (water free) followed by cold PBS to reach a final concentration of 5 µM. The tubes were then incubated for 24 hours at 4ºC to allow for oligomerization. Later, the mix was spinned down and the supernatant was extracted.

Behavioral assays
Spatial memory was tested in a Morris water maze setup as described previously (Hijazi et al., 2019). Briefly, mice were trained for 4 consecutive days with 4 trials per day. In every trial, mice were put in the water at a random start position and were given a maximum of 60 s to reach the platform. To avoid hypothermia, mice were assigned back to their home cage for 3 min after 2 trials. On day 5, the platform was removed and a probe trial was conducted. Mice were placed in the pool opposite from the platform location and were given 60 s to explore the water. The latency to find the platform was measured during training and the time spent in each quadrant of the pool was measured in the probe trial. Memory was evaluated as the percentage of time spent in the target quadrant.

Data collection and statistical analysis
Sample sizes were selected based on small pilot studies and previous experiments. The following statistical tests were performed: Student's t-test for two-group comparison for groups with equal variances, a Wilcoxon-Mann-Whitney rank test for two-group comparison of non-parametric data with unequal variances and two-way repeated measures ANOVA for assessing effects within groups and between groups in all experiments with repeated measurements in the same cell or animal. All tests were two-sided. All quantitative data are represented as means ± standard errors of the means (SEM). All mice were randomly assigned to the different groups to reduce selection bias. Experimenters were blind to the treatment and group of mice for all experiments.

Supplemental References

Hijazi, S., Heistek, T.S., Scheltens, P., Neumann, U., Shimshek, D.R., Mansvelder, H.D., Smit, A.B., and van Kesteren, R.E. (2019). Early restoration of parvalbumin interneuron activity prevents memory loss and network hyperexcitability in a mouse model of Alzheimer's disease. Mol Psychiatry.

Hippenmeyer, S., Vrieseling, E., Sigrist, M., Portmann, T., Laengle, C., Ladle, D.R., and Arber, S. (2005). A developmental switch in the response of DRG neurons to ETS transcription factor signaling. PLoS Biol *3*, e159.

Stine, W.B., Jungbauer, L., Yu, C., and LaDu, M.J. (2011). Preparing synthetic Abeta in different aggregation states. Methods Mol Biol *670*, 13-32.

Vegh, M.J., Heldring, C.M., Kamphuis, W., Hijazi, S., Timmerman, A.J., Li, K., van Nierop, P., Mansvelder, H.D., Hol, E.M., Smit, A.B.*, et al.* (2014). Reducing hippocampal extracellular matrix reverses early memory deficits in a mouse model of Alzheimer inverted question marks disease. Acta neuropathologica communications *2*, 76.